AIMS Materials Science, 4(5): 1122-1139.
DOI: 10.3934/matersci.2017.5.1122
Received: 26 July 2017
Accepted: 26 October 2017
Published: 01 November 2017

http://www.aimspress.com/journal/Materials

Research article

Synthesis and characterization of organic montmorillonite-polyvinyl alcohol-co-polyacrylic nanocomposite hydrogel for heavy metal uptake in water

Mona Mohsen [1], Ehsan Gomaa [1,*], Nabila Ahmed Mazaid [2], and Reem Mohammed [1]

[1] Physics Department, Faculty of Science, Ain Shams University, Abbassia, 11566, Cairo, Egypt
[2] Polymer Chemistry Department—National Center for Radiation Research and Technology, Atomic Energy Authority, Egypt

* **Correspondence:** Email: ehsan.gomaa53@gmail.com.

Abstract: In the present work, preparation of organic montmorillonite-polyvinyl alcohol-co-polyacrylic (OMMT-PVA/AAc) nanocomposite hydrogels are performed with different OMMT ratios ranging from 1.3 to 15% using γ irradiation as initiator to induce crosslink network structure. These nanocomposites hydrogels are prepared to use in heavy metals water decontamination. The effect of clay ratio and absorbed dose on gel fraction and swelling% has been investigated. It is found that the gel fraction increases up to 92% with increasing the loaded OMMT to 15%, whereas the swelling% reaches its maximum value at a ratio of nanoscale clay of 6% and at an absorbed dose of 4 kGy. The thermal stability of PVA/AAc hydrogel and OMMT-PVA/AAc nanocomposite hydrogels has been determined by thermogravimetric analysis (TGA), which indicated a higher thermal stability of the nanocomposite hydrogel. The FTIR spectral analysis has identified the bond structure of the PVA/AAc hydrogel and the OMMT-PVA/AAc nanocomposite. The nanostructure of the composite as well as the degree of exfoliation of clay are studied by X-ray diffraction (XRD). Its free volume holes parameters (size and fraction) are investigated by means of positron annihilation lifetime spectroscopy (PALS).

After loading the bulk and nanocomposites hydrogels with different heavy metals (Cu^{2+}, Co^{2+} and Ni^{2+}), UV spectroscopy is applied to determine the metal ion concentration before and after treatment. The distribution of heavy metals on the hydrogels is determined by energy dispersive X-ray (EDX). The factors affecting the heavy metal uptake, such as contact time, pH and metal ion concentration of solutions are studied.

The results have shown that, the presence of OMMT increases the thermal stability of PVA/AAc

due to the hydrogen bond formed between them which, is confirmed by FTIR. In addition, the resulting gel fraction after irradiation with relatively low gamma absorbed dose increased by 120%, enabling the sample to be reused for several times. In addition, the metal adsorption has increased from 194, 185, 144 mg/g for Cu^{2+}, Co^{2+} and Ni^{2+} respectively in case of previously prepared PVA/AAc hydrogel to 835, 785, 636 mg/g for Cu^{2+}, Co^{2+} and Ni^{2+} respectively for OMMT-PVA/AAc nanocomposite.

Keyword: hydrogels; montmorillonite; nanocomposite; metal uptake; free-volume

1. Introduction

Heavy metals have specific density of more than 5 g/cm^3 such as copper, cobalt, iron, manganese, chromium, nickel, gold, and lead [1]. Although most of these metals have important human bodily functions, their absorption in high amounts may cause serious health effects as cholera, cancer, diseases of the kidneys, the circulatory system, the nervous system and can damage the fetal brain. Adsorption on hydrogels is the most practical technique used for removal of such heavy metals [2].

Hydrogels are three-dimension hydrophilic polymeric materials. They have many advantages such as swelling without dissolving, very sensitive for change in temperature and pH, selective adsorbent material and easy modified to fit in many applications [3].

To increase the thermal stability and the metal adsorption amount, nanocomposite hydrogels are prepared [4,5]. These are reinforced three dimensions' networks, which consist of a cross-linked hydrophilic polymer matrix and nanoscale-reinforcing agent [6]. The most reinforcing agent used is clay, such as montmorillonite, rectonite, hectorite, etc. [7,8,9].

Burham et al. [10] prepared bentonitic clay samples and found that, the maximum adsorption capacities were 8.2 and 9.45 mg/g for Cd^{2+} and Zn^{2+}, respectively. Rafiei et al. [11] prepared Bentonite samples and PAA-Bentonite for the removal of Pb(II) ions. They found that, the percentage of the Pb(II) removal was 82.31% for the Bent sample and 99.43% for PAA-Bent nanocomposite. Ilgin et al. [12] found that, using p(AAm-co-METAC)/MMT composite hydrogel the maximum adsorption capacities were 320, 285, 240 and 120 mg/g for $Zn^{2+} > Ni^{2+} > Cu^{2+} > Pb^{2+}$, respectively. Mahaweero et al. [13] prepared novel chitosan (CTS)/montmorillonite (MMT) hybrid hydrogels for the removal of Cu(II), and found that, the maximum adsorption capacities at pH = 3, 7 and 10 are 286, 282 and 179 mg/g, respectively. Zhu et al. [14] prepared Chitosan co montmorillonite and found that, adsorption of Cd is in the range of 10 mg/g. Sirousazar et al. [15] prepared polyvinyl alcohol nanocomposite hydrogels with natural Na-montmorillonite. They found that, the gel fraction of nanocomposite hydrogels containing 15 wt% of MMT has been enhanced by 17.1%, as compared to pure hydrogel.

In our previous work[16], PVA/AAc hydrogel was prepared for the removal of different heavy metals. A maximum swelling percent is obtained at gel fraction 82% and absorbed dose of 20 kGy. The adsorption amount was found to be 194 > 185 > 144 mg/g for $Cu^{2+} > Co^{2+} > Ni^{2+}$ respectively after 24 h treatment time.

The aim of the present work is to enhance the heavy metal adsorption capacity of PVA/AAc hydrogel by preparing a nanocomposite hydrogel of OMMT-PVA/AAc consisting of a cross-linked

hydrophilic PVA/AAc matrix and nanoscale-OMMT reinforcing agent. The nanocomposite hydrogel is prepared by gamma irradiation and the effect of different OMMT ratios on gel fraction and swelling percentage is studied. We have chosen organic montmorillonite for its super adsorption property for water, high surface area, high mechanical and thermal stability, low cost and it can be used as crosslinker [10]. The degree of exfoliated-intercalated is examined by XRD while EDX illustrate respectively the competitive adsorption and morphology of the PVA/AAc and nanocomposite hydrogels. The effect of OMMT on thermal stability is studied by TGA. Furthermore, the bond structure and free volume nanostructure is examined by FTIR and PALS respectively. The factors affecting the adsorption amount such as treatment time, pH and metal ion concentration of solutions are determined.

2. Materials and Method

2.1. Materials

Acrylic acid (AAc) is purchased from (Merck Germany), whereas polyvinyl alcohol (PVA) powder is purchased from Aldrich Company, having an average molecular weight (MW) of 15,000. Pure sodium montmorillonite (Na^+-MMT) with a cation-exchange capacity (CEC) of 90 mmol/100 g is supplied by International Company for Mining and Investments (ICMI), Cairo, Egypt.

Cetyltrimethylammonium bromide (CTAB) with chemical formula—$CH_3(CH_2)_{15}N(CH_3)_3Br$, which is used as a surfactant, is purchased from Indian supplier of laboratory chemicals in Delhi, India.

The other chemicals, such as citric acid, sodium di-hydrogen phosphate buffer analytical reagent as well as the metals as cobalt sulphate, copper sulphate and nickel sulphate have been purchased from EL-Nasr Company for Chemical Industries, Cairo, Egypt and used without further purification.

2.2. Gamma Irradiation

The samples are irradiated with ^{60}Co at the Russian irradiation facility gamma rays source with a dose rate of 2.08 kGy/h at National Center for Radiation Research and Technology, Atomic Energy Authority, Egypt.

2.3. Treatment of Clay (MMT)

25 g of MMT with 800 ml of distilled water at 80 ℃ and 10 g CTAB are vigorously stirred of for 2 hours by a magnetic stirrer. To completely remove the bromide ions, the precipitate was filtered and washed several times with hot distilled water then dried at 60 ℃ for 24 hrs. The organophilic montmorillonite (OMMT) is ground in a mortar and the particles of size less than 75 μm were collected.

2.4. Preparation of the Nanocomposite Hydrogel OMMT-PVA/AAc

OMMT-PVA/AAc is prepared according to the following procedures: first, a stock PVA solution

with 5% concentration is prepared by adding 5 g of PVA in 100 mL distilled water. Some amount of this solution is added to an amount of AAc solution and 50 ml distilled water and then stirred for 10 min. The mixture is transferred into a six-necked flask equipped with a stirrer. A stock solution of OMMT 1% concentration is prepared. Then different ratios (0, 1.3, 6, 7, 10, and 15%) of OMMT is dispersed in the above-mentioned PVA-AAc mixed solution and stirred vigorously for 24 h to achieve complete mixing. Finally, the flasks are irradiated at absorbed dose 4 kGy at dose rate 2.08 kGy/h, and the gels soaked in betri dish. Films of PVA/AAc hydrogel and PVA/AAc-OMMT nanocomposites of 1 mm thickness are then formed.

2.5. Preparation of Buffer Solution of Different pH Values

Buffer solutions are prepared with pH values ranged from 2–12, using 0.2 M sodium dihydrogen phosphate/disodium hydrogen phosphate and 0.2 M Citric acid/disodium citrate.

2.6. Gel Determination in the Hydrogels

The obtained hydrogels are weighted (W_g), then soaked in distilled water for 24 hrs at 100 ℃, to remove the unreacted monomers. The hydrogels are then dried in a vacuum and reweighted (W_d). The gel fraction of the hydrogel is determined by the following equation:

$$Gel\% = \frac{W_g}{W_d} \times 100 \tag{1}$$

where, W_g and W_d represent the weights of the gelled and dry hydrogel respectively.

2.7. Swelling Measurements

Fixed weight of the dried gel (W_0) is soaked in distilled water at room temperature for 24 hrs. The gel is removed and the excess water on the surface is removed with filter paper and reweighted. The swelling ratio is calculated as follows

$$Swelling\% = \frac{W_t - W_0}{W_0} \times 100 \tag{2}$$

W_t is the weight of swollen gel sample at time t, W_0 is the initial weight of dry gel samples.

2.8. Characterization

Positron annihilation lifetime (PAL) measurements were carried out at room temperature using a fast-fast coincidence system with time resolution of 250 ps (full width at half-maximum, FWHM). A 11 μCi ^{22}Na positron source is deposited on Kapton foils (thickness less than 1 mg/cm^2) and sandwich between two identical pieces of the sample. The lifetime spectra were accumulated to a total of 5×10^6 counts and then analyzed using the computer program LT 9.0 [17]. Three lifetime components were obtained: the lifetime and intensity (τ_1 & I_1) of para-positronium (p-Ps), the lifetime and intensity of free positron (τ_2 & I_2) and the lifetime and intensity for the ortho-

positronium (o-Ps) (τ_3 & I_3), which is due to pick-off annihilation in free volumes. The mean free-volume radius (R) of holes can be calculated by using the following semi empirical equation [18,19].

$$\tau_3 = 0.5\left[1 - \frac{R}{R+\Delta R} + \frac{1}{2\pi}\sin\left(\frac{2\pi R}{R+\Delta R}\right)\right]^{-1} \quad (3)$$

where ΔR = 1.66 Å is the fitted empirical electron-layer thickness [19].

By fitting the above equation with the measured τ_3, values of R and $V_h = \frac{4}{3}\pi R^3$ can be calculated (where the free-volume holes are assumed to be spherical). The relative intensity of the longest component, I_3, is generally correlated to the fractions of holes which can be considered as trapping centers for Ps. A semi-empirical relation may be used to determine the relative fraction of the free-volume holes (F%) in polymers [19] as follows:

$$F = V_h I_3 \quad (4)$$

X-ray diffraction (XRD) measurements are performed by means of a Bruker D2 Phaser Diffractmeter (30 kV, 10 mA) with Cu Kα radiation. The elemental analyses of the hydrogels are evaluated by Energy Dispersive X-ray spectroscopy (EDX) at an accelerating voltage between 0 and 20 keV by using X-ray diffractometer (PW1390) from Philips.

Fourier transform infrared (FTIR) spectra are recorded on Mattson 1000 spectrometer using pressed KBr pellets. UV-vis Pye Unicam Spectrophotometer Type SP 8-200 is used to determine the metal ion concentration before and after treatment at room temperature. Thermogravimetric (TG) analyses are carried out using A Shemadizu TGA-50 system with nitrogen atmosphere, the samples are heated from 30 to 1000 °C at a heating rate (20 ml/min) in airflow. The clay content in the dried hydrogel is evaluated from the residual weight at 1000 °C. The pH of the solution is determined using Huawei pH meter.

2.9. Metal Uptake Measurements

The fixed weight (0.5 g) of the prepared hydrogel is immersed in metal feed (100 ml) solutions of a definite concentration. The concentrations of metal ions before and after the treatment are determined by ultraviolet spectroscopy (UV) and used for the calibration process. The pH and temperature of the metal feed solutions are adjusted before it is applied for treatment processes. The adsorption amount (E) is calculated as.

$$E\ (\text{mg/g}) = \frac{\text{V}\,(\text{C}_\text{i} - C_t)}{W} \quad (5)$$

where, V is the volume of solution (L), W is the weight of the hydrogel (g). Whereas, C_i, and C_r are the concentrations of metal ions in mg/L before and after the adsorption, respectively.

2.10. Factors Affecting the Adsorption Amount

The pH dependence is performed by mixing 0.5 g of the hydrogel samples with 100 ml of 1000 ppm (mg/l) metal ion solutions for 24 h.

The effect of contact time is determined by using a fixed weight of the hydrogel (0.5 g), to be mixed in a solution with 100 ppm with fixed pH, at regular time intervals.

The effect of initial metal ion concentration is measured by using a fixed weight of the hydrogels (0.5 g) to be put with a series of different metal ion concentrations at fixed pH and for fixed time.

3. Results and Discussion

3.1. Effect of OMMT on Gel Fraction and Swelling Percent of Nanocomposite Hydrogel

The dependence of the gel fraction of the nanocomposite hydrogel on the ratio of OMMT is illustrated in Figure 1. It is found that the gel fraction increases from 44 to 85% by increasing the ratio of OMMT to 6%. Since the gel fraction shows weak increase at higher OMMT amount therefore, 6% OMMT is applied to synthesize the samples for heavy metal uptake. The increase in gel fraction can be explained as follows: addition of the organic OMMT leads to a strong hydrogen bond interaction between its function groups (OH) and the PVA/AAc hydrogel matrix. Thus, producing a three-dimensional nanocomposite which has been confirmed by FTIR indicates that OMMT acts as a crosslinker for hydrogel, in agreement with Kokabi et al. [20] and Sirousazar et al. [15]. It is to be mentioned, that the main disadvantage of PVA/AAc is the low gel fraction, which leads to a high solubility in water, thus reducing the adsorption efficiency.

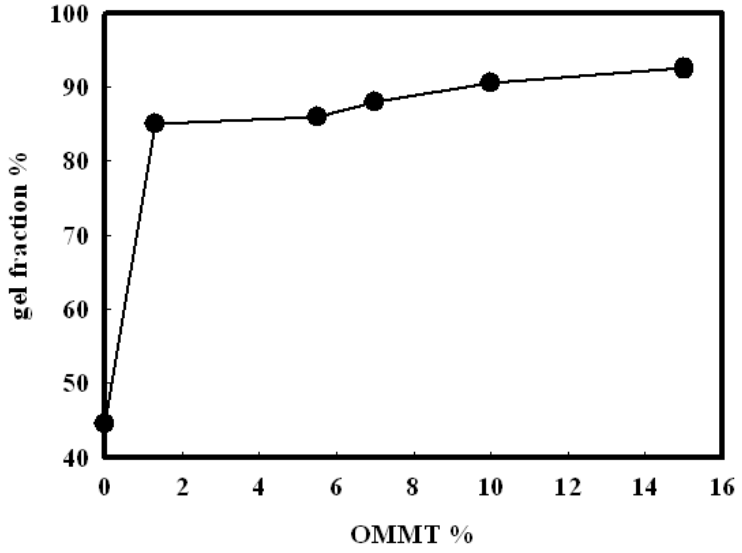

Figure 1. Effect of different OMMT ratios on the gel fraction of the nanocomposite hydrogel.

Figure 2 shows the effect of OMMT ratio on the swelling%, which increases by increasing the OMMT up to 6% then decreases. The initial increase of swelling is due to its the large hydrophilicity

of OMMT and the expansion of the network making the diffusion of water easier [21,22]. Therefore, OMMT-PVA/AAc gained lager hydrophilicity, with increasing OMMT ratio in nanocmposites. This is due to nano size and has high surface area of OMMT as well as the presence of sodium as the predominant exchangeable cation can result in the clay swelling to several times its original volume.

On the other hand, the sheets of the clay are expected to be well-dispersed in the hydrogel, leading to the formation of pores which leads to a decrease in the crosslink density between the OH group of OMMT and PVA/AAc chains. But with the increase of OMMT ratios and as it has a high cation exchange capacity, hydrogen bonding and silanol groups (–Si–OH) in its structure so these leads to increase in stability of therefore OMMT act as co-crosslinker.

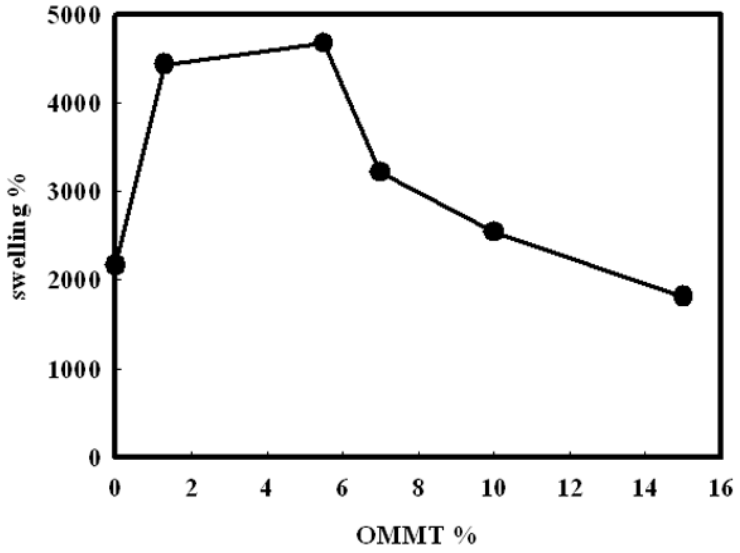

Figure 2. Effect of different OMMT ratios on the swelling% of hydrogel nanocomposite at absorbed dose 4 kGy.

The decrease of swelling% at clay ratio larger than 6% can be explained by the increase of the crosslink density which restricts the mobility of the hydrogel chains and thus producing smaller sized pores. In addition, it is expected that, the silicate layers act as a physical barrier against the diffusion of water molecules [21,23].

3.2. Effect of Different Absorbed Dose on Gel Fraction and Swelling of Nanocomposite (OMMT-PVA/AAc)

The effect of absorbed dose on gel fraction and swelling% is illustrated in Figures 3 and 4. Figure 3 shows that the gel fraction increases from 72 to 95% with increasing absorbed dose from 2 to 8 kGy then remains constant at higher dose. This is due to the increase in the crosslinking between hydrogel and OMMT [24].

On the other hand, the swelling percent reaches a maximum at 4 kGy and then decreases as shown in Figure 4. Accordingly, the OMMT-PVA/AAc nanocomposite are prepared using 4 kGy γ-absorbed dose and with 6% OMMT.

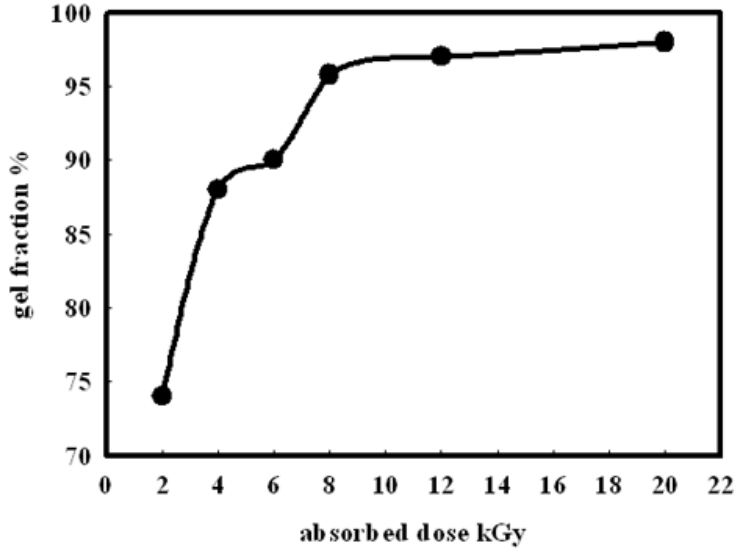

Figure 3. Effect of absorbed dose on the gel fraction of nanocomposite with 6% OMMT.

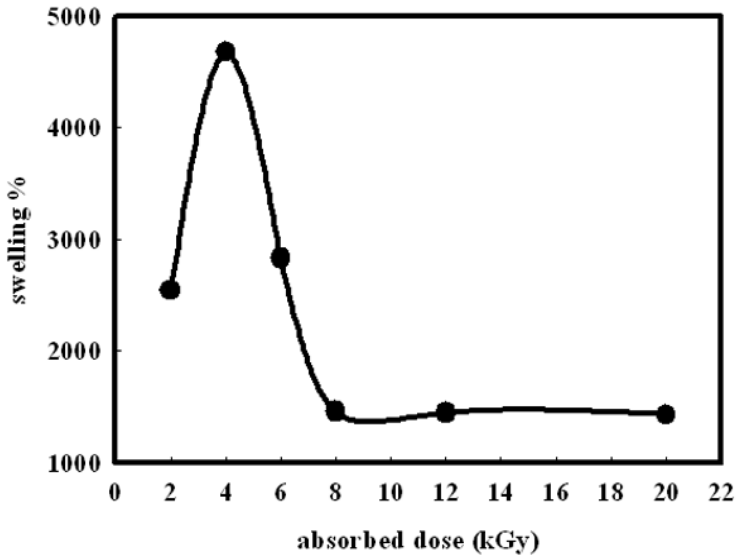

Figure 4. Effect of absorbed dose on the swelling percent of nanocomposite with 6% OMMT.

3.3. Characterization of the Selected Nanocomposite Hydrogel

3.3.1. FTIR Analysis

The FTIR analysis is used to examine the functional and bond structure of PVA/AAc, OMMT and (OMMT-PVA/AAc) as demonstrated in Figure 5. In Figure 5(a), there is a broad band at 3460 cm^{-1} corresponding to overlapping between OH stretching of carboxylic group of AAc with alcoholic OH of PVA. The stretching vibration band at 1090 cm^{-1} is attributed to an esterification reaction between the carboxylic group of AAc and a hydroxyl group of PVA. In Figure 5(b), the broad band at 3419 cm^{-1} is due to OH stretching of interlayer water. The OH stretching bands at

3697 cm^{-1} and 3623 cm^{-1} indicate AL–OH and Si–OH respectively. The C–H asymmetric and symmetric stretching vibrational bands of surfactant (CTAB) appear at 2920 cm^{-1} and 2850 cm^{-1} respectively. The peak at 1644 cm^{-1} is due to OH bending in the water. The stretching vibrational peak at 1034 cm^{-1} is attributed to Si–O of silicate layers. The bending vibration of OH in Al_2OH is observed at 912 cm^{-1}. The bending vibrational at 525 cm^{-1} and 467 cm^{-1} are due to Si–O–Al and Si–O–Si respectively. Figure 5(c) shows the shift of the OH peak of hydrogel to 3419 cm^{-1}, which is attributed to strong interaction (formation of hydrogen bonds) between OH groups of the PVA/AAc hydrogel and the OMMT organoclay. The appearance of organoclay peaks, and their shift indicate the presence of OMMT clay in the nanocomposite. These results confirm the crosslinking reaction between functional groups of silicate layers and hydrogel chains [14,20].

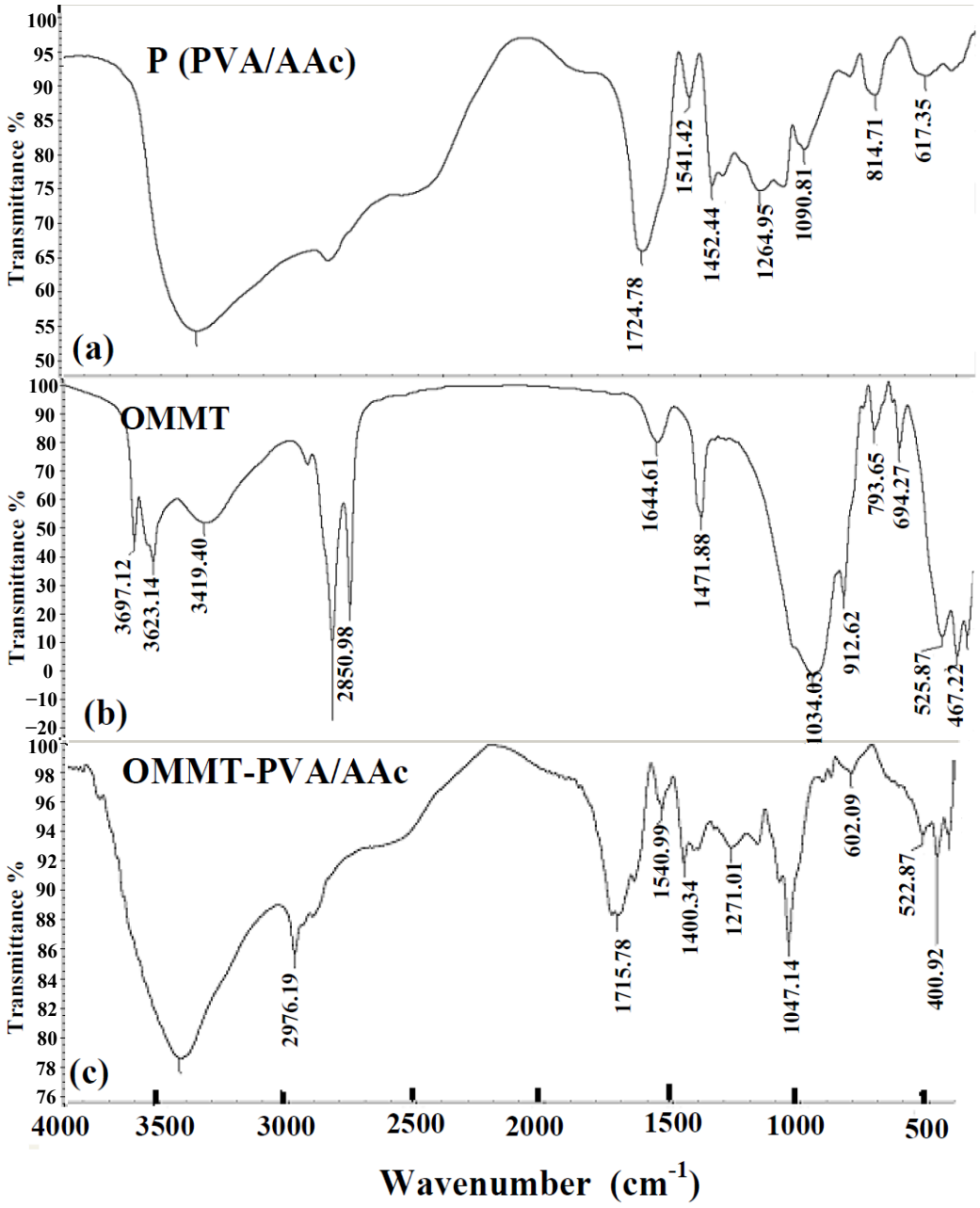

Figure 5. FTIR spectra of (a) PVA/AAc hydrogel, (b) OMMT and (c) OMMT-PVA/AAc hydrogel nanocomposite.

3.3.2. Microstructure Analysis by XRD

Figure 6 illustrates the XRD patterns of PVA/AAc hydrogel, OMMT and OMMT-PVA/AAc nanocomposite hydrogel. Pure hydrogel pattern does not show any sharp peaks, with only a broad peak in the 2θ at 20° to the polymer networks and show the amorphous structure of hydrogel. The pattern of OMMT shows a polycrystalline structure due to the existence of sharp peaks. There is a crystalline diffraction peak at 2θ = 5.8°, which corresponds to a d-spacing of 15.1 Å. In addition, there are two other peaks at around 2θ = 21° and 27°, which may be due to the impurities inside the clay. On the other hand, there is no peak for clay in the OMMT-PVA/AAc pattern, which indicates that the regular structure of the OMMT is destroyed due to its complete dispersion in the PVA/AAc matrix, forming exfoliated structure in agreement with Kokabi et al. [13,20,25] and Usuki et al. [26].

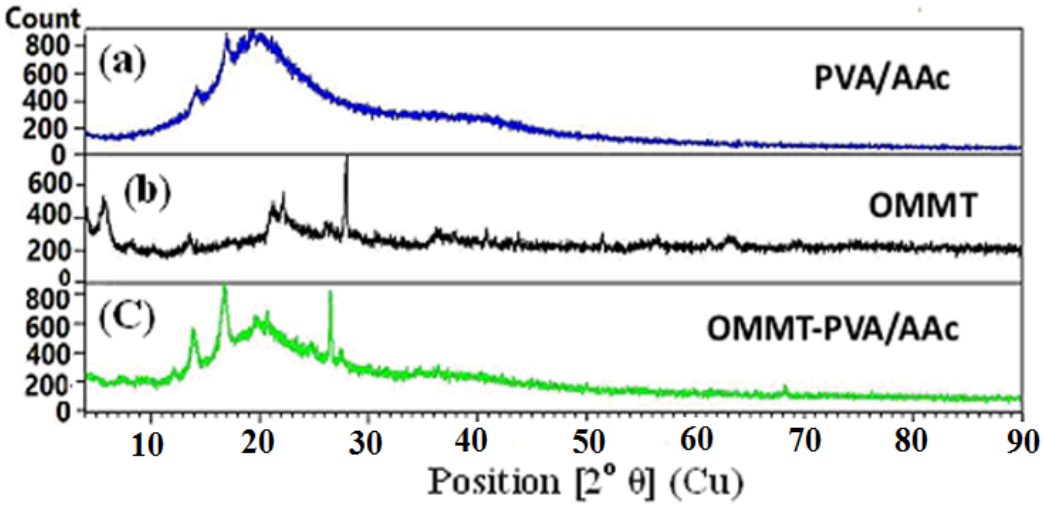

Figure 6. XRD patterns of (a) PVA/AAc (b) OMMT and (c) OMMT-PVA/AAc.

3.3.3. Free-volume Nanostructure by Positron Annihilation Lifetime Spectroscopy

Figure 7 shows the variation of o-Ps lifetime components (τ_3 and I_3), and free-volume parameters (V_h and F%) as a function of (OMMT) ratio. The free volumes V_h shows a maximum at 4% OMMT, where V_h increases from 55 $Å^3$ to 65 $Å^3$ which explains the maximum obtained in swelling%. At 7% OMMT a decrease in V_h is observed without major change in its fractions (F%), which can be explained by a possible chain segment immobilization. Increasing the clay to 11% which leads to an increase in V_h to 70 $Å^3$ is due to the creation of interfacial regions thus enhancing the size of free volume and decreasing its fractions, F%.

The variation of free volumes parameters (τ_3 & V_h) and (I_3 & F%) according to the absorbed dose mainly depends on the degree of crosslinking density of the polymeric chain. From Figure 8, it is clear that both the free-volume size and its fraction decrease at absorbed dose 4 kGy, which may be due to the close packing of the polymeric chain, which leads to increase in the entanglement of the polymer chains and increase in crosslinking density. Consequently, this leads to a decrease in the size and fraction of free-volume holes (V_h and F%).

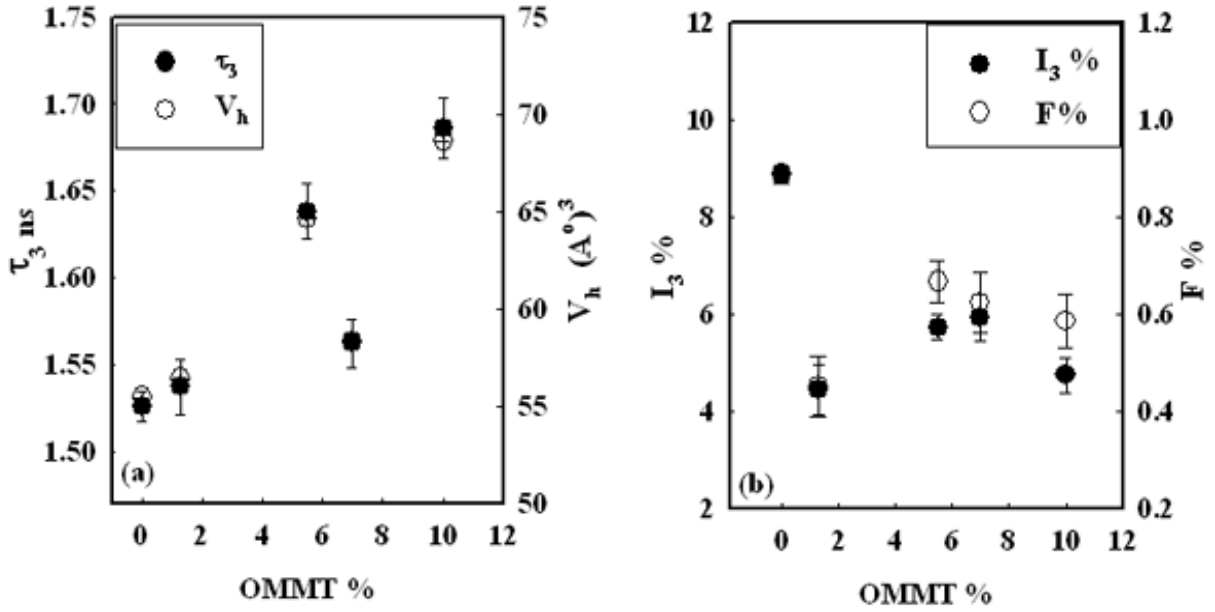

Figure 7. The effect of OMMT% on (a) size of free-volume holes (τ_3 and V_h) and (b) fraction of free-volume holes (I_3 and F%) of nanocomposite hydrogel at 4 kGy absorbed dose.

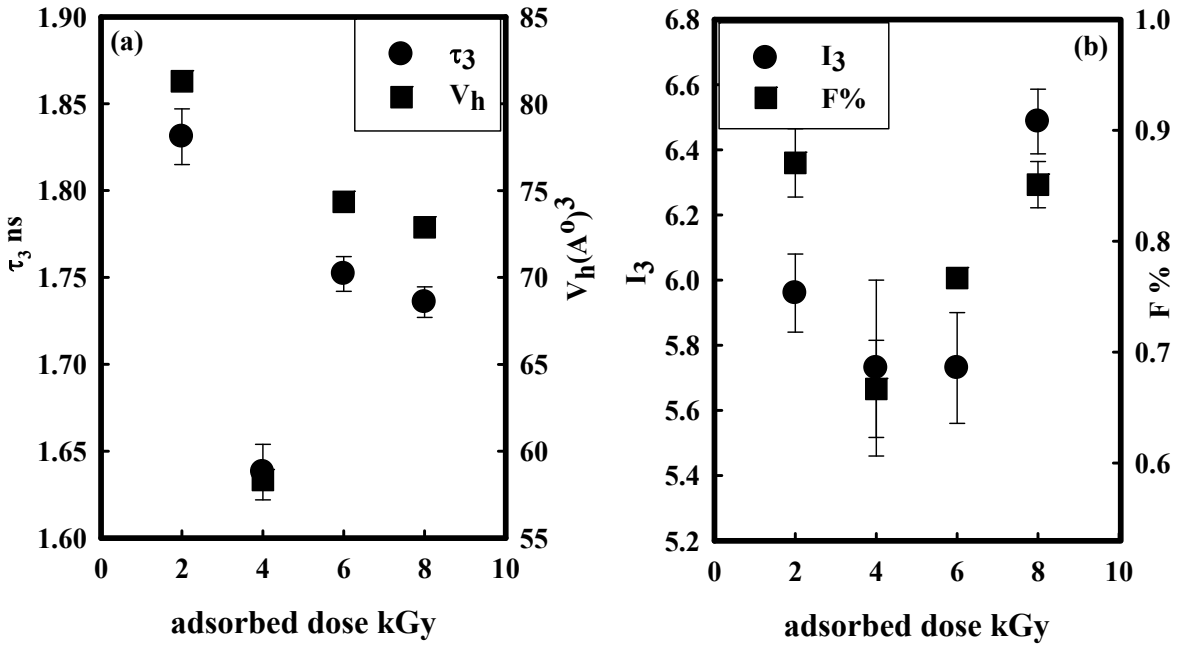

Figure 8. The effect of absorbed dose on (a) size of free-volume holes (τ_3 and V_h) and (b) fraction of free-volume holes (I_3 and F%) of nanocomposite with 6% OMMT.

At dose, higher than 4 kGy an increase in free-volume hole size and its fraction is observed. This increase is due to the scissoring of polymeric chains.

Figure 9 illustrates a positive correlation between swelling% and free-volume parameters (V_h and F%) as a function of OMMT ratio. One can conclude that the free volume size and its fraction play a major role in the swelling mechanism.

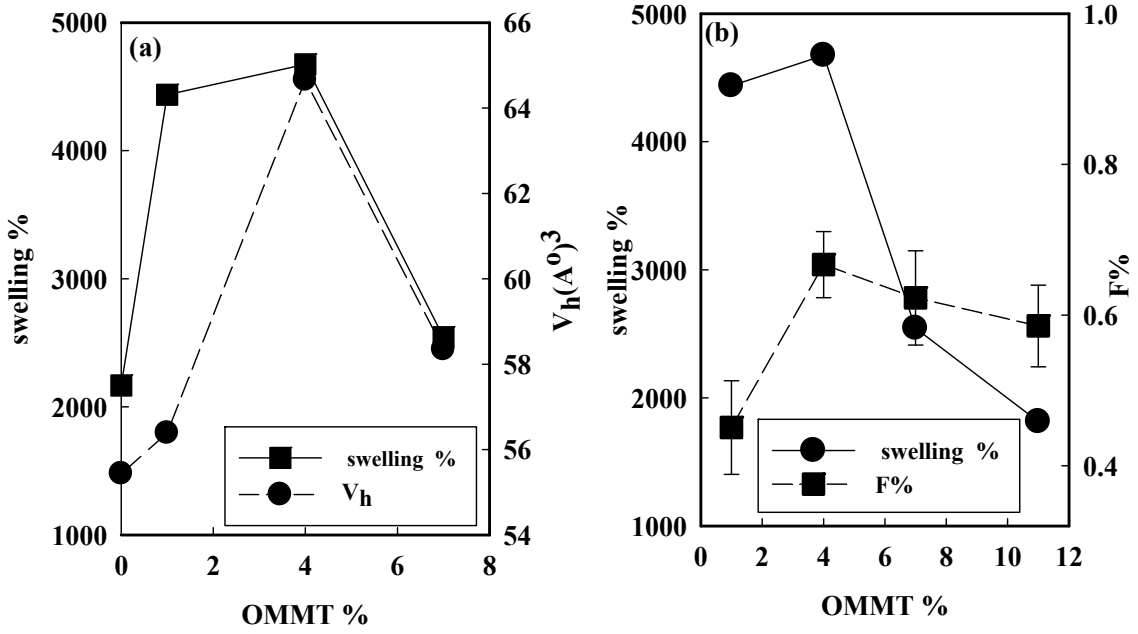

Figure 9. Correlation of swelling percent with (a) size of free-volume holes and (b) fraction of free-volume holes. (V_h and F%) as a function of OMMT%. (The lines are only drawn to guide the eye).

3.3.4. Thermal Gravimetrical Analysis

Thermal gravimetrical analysis (TGA) is used to study the thermal stability and degradation temperature of the PVA/AAc hydrogel and OMMT-PVA/AAc nanocomposite hydrogel and that adsorbed with metal ions (Cu^{2+}). Samples are heated with heating rate of 10 ℃/min at temperature range from 30 to 650 ℃ under flow of nitrogen with flowing rate of 20 ml/min. As shown in Figure 10, the thermal stability of nanocomposites hydrogel is higher than that of PVA/AAc hydrogel. This is due to the silanol group on clay structure and the hydrogen bond which is formed between hydrogel and clay layers. This leads to a decrease in the chain mobility and increase in the thermal stability [27]. Adsorption of Cu^{2+} on the nanocomposite hydrogel leads to an increase in its thermal stability due to the complexation formed between them. As shown in Figure 10, there are three degradation stages: the first stage is due to vaporization of water in the structure, the second stage is due to degradation of functional groups in the side chains and the third is due to the degradation of the backbone chain [3,23,24]. It is found that after heating to 600 ℃, the weight remaining of nanocomposite hydrogel is higher than that of hydrogel as shown in Table 1.

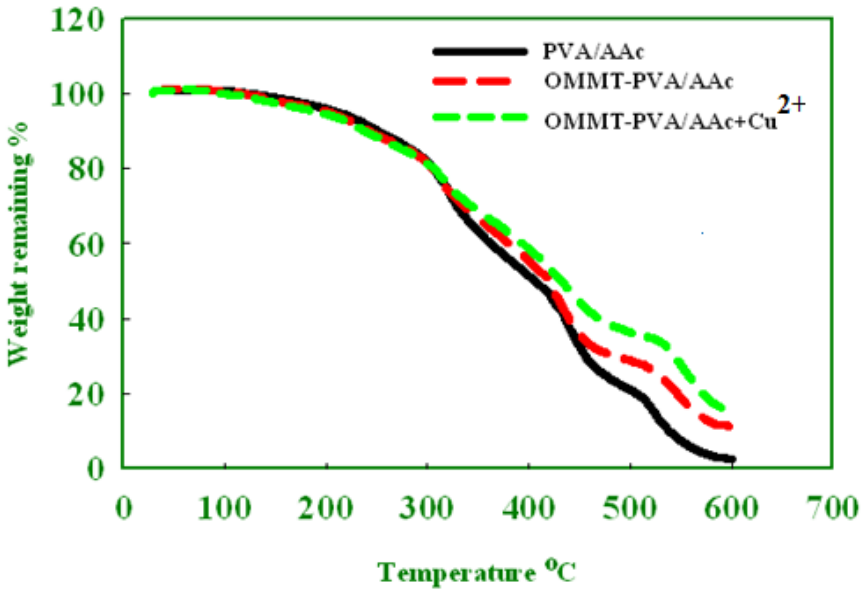

Figure 10. TGA of PVA/AAc hydrogel and OMMT-PVA/AAc nanocomposite hydrogel and those adsorbed with different Cu^{2+} ions.

Table 1. The different decomposition stages with percentage weight loss for hydrogel and nanocomposite hydrogel at absorbed dose 4 kGy.

	T(Onset)-T(Endset)	Weight loss %	T(Onset)-T(Endset)	Weight loss %	T(Onset)-T(Endset)	Weight loss %	Weight remaining after 600 ℃
PVA/AAc	301–334 ℃	23%	436–455 ℃	26%	527–548 ℃	19%	32%
OMMT-PVA/AAc	311–332 ℃	18%	431–455 ℃	15%	532–579 ℃	16%	50%
OMMT-PVA/AAc + Cu^{2+}	299–333 ℃	13%			533–576 ℃	19%	66%

3.4. Application of the Prepared PVA/AAc and OMMT-PVA/AAc Hydrogels in Heavy Metal Uptake

3.4.1. Effect of Metal Ion Concentration

Figure 11 illustrates that, the adsorption amount for nanocomposite hydrogel reaches a maximum at 100 ppm for both Cu^{2+} and Co^{2+} ions wheras for Ni^{2+} it reaches the maximum at 250 ppm. At higher concentrations, a decrease in the adsorption amount is observed for all metals. This is due to the fact that, at low concentrations the adsorption sites are highly effective and active, which facilitate the diffusion of ions [27]. This figure aslo shows that the maximum adsorption amounts for nanocomposite hydrogel is 650 mg/g, 625 mg/g and 512 mg/g for Cu^{2+}, Co^{2+} and Ni^{2+} respectively, and following the order $Cu^{2+} > Co^{2+} > Ni^{2+}$ in agreement with El Din et al. [23]. In the present study the metal ion concentration will be fixed at 100 ppm.

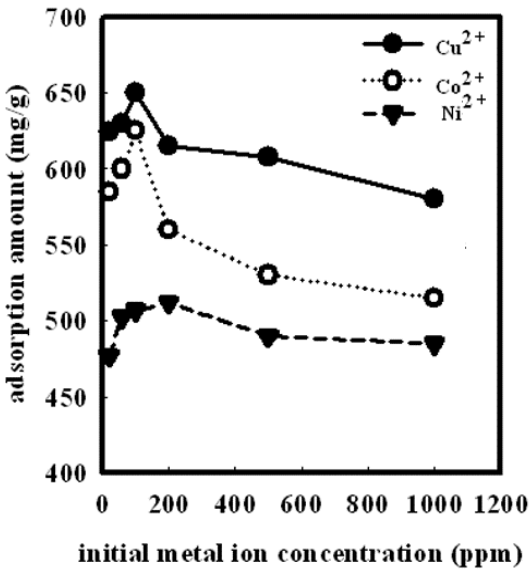

Figure 11. Effect of initial metal ion concentration of adsorption amount of different metals onto nanocomposite hydrogel.

3.4.2. Effect of Contact Time

Figures 12 shows the influence of treatment time on the adsorption amount of different metals onto PVA/AAc and OMMT-PVA/AAc hydrogels at concentration of 100 ppm. It is found that the adsorption amount increases by increasing contact time up to 2 hrs and then remains constant due to the saturation of the active adsorption centers. The adsorption amount follows the same order namely $Cu^{2+} > Co^{2+} > Ni^{2+}$.

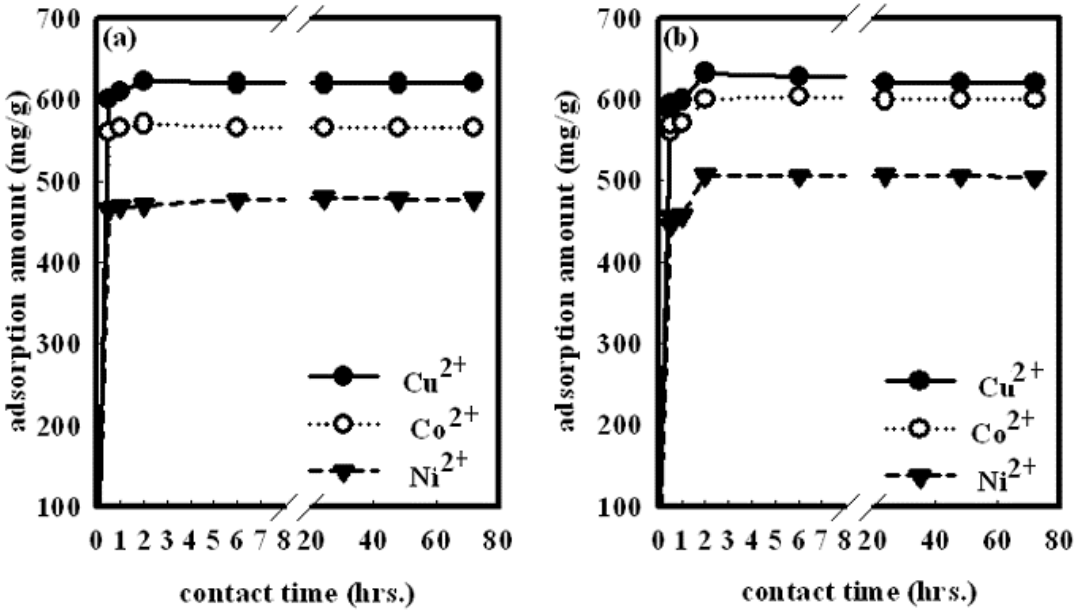

Figure 12. Effect of contact time on adsorption amount for different metals onto (a) PVA/AAc and (b) nanocomposite hydrogel.

3.4.3. Effect of pH of the Solution

The effect of pH on the adsorption amount of PVA/AAc and OMMT-PVA/AAc nanocomposite hydrogels at metal ion concentration of 100 ppm and after 2 hrs are illustrated in Figure 13. At pH = 5, the adsorption amount reaches a maximum for the three metals.

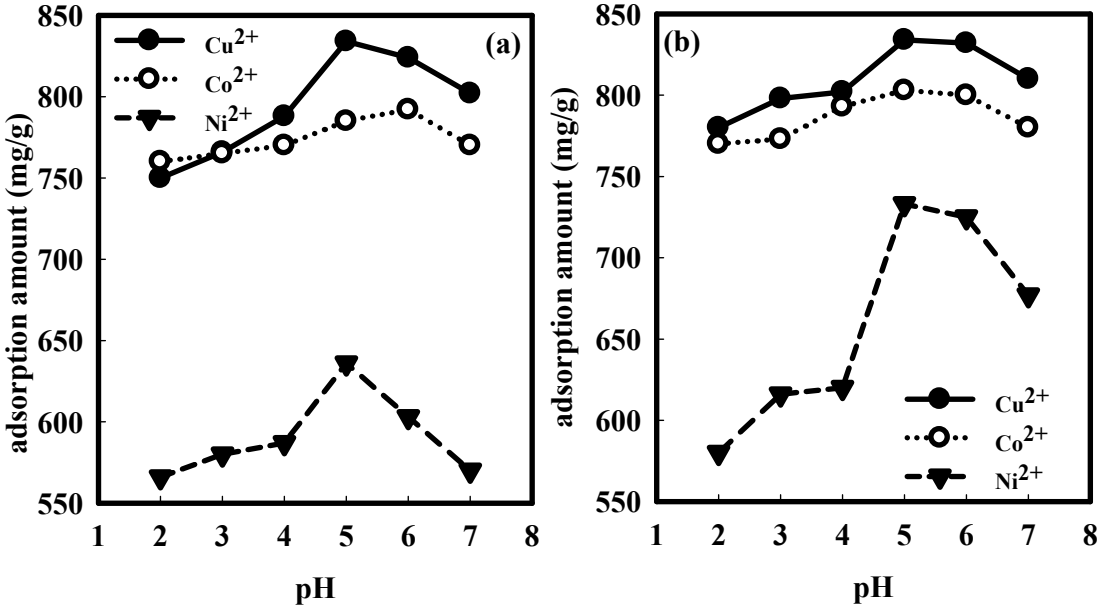

Figure 13. Effect of pH of the metal solution on adsorption amount of different metals on (a) PVA/PAAc and (b) nanocomposite hydrogel.

3.5. Energy Dispersive X-ray Analysis

The hydrogel and nanocomposite hydrogel adsorb the three different metals by the order of $Cu^{2+} > Co^{2+} > Ni^{2+}$ as illustrated in Figure 14. Table 2 demonstrates the high affinity and selectivity of OMMT-PVA/AAc to only Cu^{2+} compared to PVA/AAc.

From Figure 14 and datas in Table 2, it is found that the hydrogel and nanocomposite uptake $Cu^{2+} > Co^{2+} > Ni^{2+}$ and OMMT improve the selectivity of Cu^{2+}.

Table 2. Affinity of hydrogel and nanocomposite hydrogel for adsorption of Cu^{2+}, Co^{2+} and Ni^{2+}.

Hydrogel		Affinity of metal uptake ratios		
		Cu^{2+}	Co^{2+}	Ni^{2+}
PVA/AAc	$Cu^{2+} > Co^{2+} > Ni^{2+}$	65.9%	18.55%	15.6%
OMMT-PVA/AAc	$Cu^{2+} > Co^{2+} > Ni^{2+}$	82.6%	8.4%	8.9%

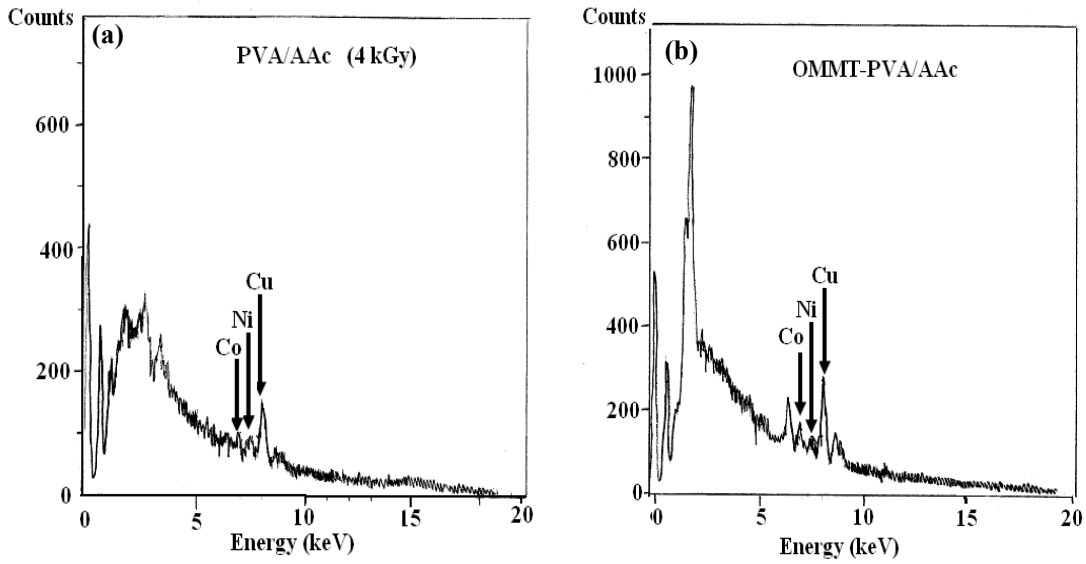

Figure 14. Affinity of (a) PVA/AAc and (b) OMMT-PVA/AAc toward Cu^{2+}, Co^{2+} and Ni^{2+} at 100 ppm.

4. Conclusion

Organic montmorillonite-polyvinyl alcohol-co-polyacrylic (OMMT-PVA/AAc) nanocomposite hydrogel has been successfully prepared by gamma-irradiation with a dose of 4 kGy, which is 5 times lower than the dose required for the preparation of PVA/AAc hydrogel and which led to an increase in the gel fraction by 120% resulting in reaching maximum adsorption amount after 2 hrs instead of 24 hrs. The microstructure and the free volume nanostructure of PVA/AAc hydrogel and OMMT-PVA/AAc nanocomposite hydrogel have been identified by XRD and PALS respectively. The bond structure has been characterized by FTIR. In addition, higher thermal stability compared to PVA/AAc hydrogel has been displayed by TGA. Furthermore, the metal adsorption has increased from 194, 185, 144 mg/g for Cu^{2+}, Co^{2+} and Ni^{2+} respectively in case of previously prepared PVA/AAc hydrogel to 835, 785, 636 mg/g for Cu^{2+}, Co^{2+} and Ni^{2+} respectively for OMMT-PVA/AAc nanocomposite hydrogel. Its affinity for Cu^{2+} metal uptake ratio is found to be 10 times higher than for Co^{2+} and Ni^{2+}. The high selectivity of the nanocomposite hydrogel follows the order of: $Cu^{2+} > Co^{2+} > Ni^{2+}$.

Conflict of Interest

No conflict of interest.

References

1. Abdel-Raouf MS, Abdul-Raheim ARM (2017) Removal of Heavy Metals from Industrial Waste Water by Biomass-Based Materials: A Review. *J Pollut Eff Cont* 5: 180.

2. Berihun D (2017) Removal of Chromium from Industrial Wastewater by Adsorption Using Coffee Husk. *J Material Sci Eng* 6: 331.
3. Chen X, Zhou S, Zhang L, et al. (2016) Adsorption of Heavy Metals by Graphene Oxide/Cellulose Hydrogel Prepared from NaOH/Urea Aqueous Solution. *Materials* 9: 582.
4. Lingamdinne LP, Kim IS, Ha JH, et al. (2017) Enhanced Adsorption Removal of Pb(II) and Cr(III) by Using Nickel Ferrite-Reduced Graphene Oxide Nanocomposite. *Metals* 7: 225.
5. Bajpai A, Tripathi N, Saxena S (2014) Nanocomposites Based on Natural Biodegradable Materials: Effect of Post-Preparative γ-Irradiation on the Swelling Properties. *Open J Org Polym Mat* 4: 10–15.
6. Pandey N, Shukla SK, Singh NB (2017) Water purification by polymer nanocomposites: an overview. *Nanocomposites* 3: 47–66.
7. El Adraa K, Georgelin T, Lambert JF, et al. (2017) Cysteine-montmorillonite composites for heavy metal cation complexation: A combined experimental and theoretical study. *Chem Eng J* 314: 406–417.
8. Akpomie KG, Dawodu FA (2016) Acid-modified montmorillonite for sorption of heavy metals from automobile effluent. *Beni-Seuf Univ J Basic Appl Sci* 5: 1–12.
9. Feng YL, Wang C, Mao N, et al. (2017) Research Progress of Organic Modified Montmorillonite. *Adv Mater* 6: 20–23. Available from: http://advinmaterials.org/article?journalid=129&doi=10.11648/j.am.20170603.11
10. Burham N, Sayed M (2016) Adsorption Behavior of Cd^{2+} and Zn^{2+} onto Natural Egyptian Bentonitic Clay. *Minerals* 6: 129.
11. Rafiei HR, Shirvani M, Ogunseitan OA (2016) Removal of lead from aqueous solutions by a poly(acrylic acid)/bentonite nanocomposite. *Appl Water Sci* 6: 331–338.
12. Ilgin P, Durak H, Gür A (2015) A Novel pH-Responsive p(AAm-co-METAC)/MMT Composite Hydrogel: Synthesis, Characterization and Its Absorption Performance on Heavy Metal Ions. *Polym-Plast Tech Eng* 54: 603–615.
13. Mahaweero T, Thanatde J (2013) Extraction of Heavy Metals from Aqueous Solutions using Chitosan/Montmorillonite Hybrid Hydrogels [PhD Dissertation]. Case Western Reserve University.
14. Zhu L, Wang L, Xu Y (2017) Chitosan and surfactant co-modified montmorillonite: A multifunctional adsorbent for contaminant removal. *Appl Clay Sci* 146: 35–42.
15. Sirousazar M, Kokabi M, Hassan ZM, et al. (2011) Dehydration kinetics of polyvinyl alcohol nanocomposite hydrogels containing Na-montmorillonite nanoclay. *Sci Iran* 8: 780–784.
16. Maziad NA, Mohsen M, Gomaa E, et al. (2015) Radiation Copolymerization of Hydrogels Based in Polyacrylic Acid/Polyvinyl Alcohol Applied in Water Treatment Processes. *J Mater Sci Eng A* 5: 381–390.
17. Kansy J (1996) Microcomputer program for analysis of positron annihilation lifetime spectra. *Nucl Instrum Meth A* 374: 235–244.
18. Schmidt M, Maurer FHJ (2000) Relation between free-volume quantities from PVT–EOS analysis and PALS. *Polymer* 41: 8419–8424.
19. Jean Y (1990) Positron annihilation spectroscopy for chemical analysis: a novel probe for microstructural analysis of polymers. *Microchem J* 42: 72–102.
20. Kokabi M, Sirousazar M, Hassan ZM (2007) PVA-Clay Nanocomposite Hydrogels for Wound Dressing. *Eur Polym J* 43: 773–781.

21. Barati A, Asgari M, Miri T, et al. (2013) Removal and Recovery of Copper and Nickel Ions from Aqueous Solution by Poly(Methacrylamide-Co-Acrylic Acid)/Montmorillonite Nanocomposites. *Environ Sci Pollut R* 20: 6242–6255.
22. Yakar A (2014) Synthesis of Poly(N-Methylol Methacrylamide/Vinyl Sulfonic Acid) Hydrogels for Heavy Metal Ion Removal. *B Korean Chem Soc* 35: 3063–3070.
23. El-Din HMN, Hegazy ESA, Ibraheim DM (2009) Synthesis and Characterization of Hydrogels Based on Gamma Irradiation of Acrylic Acid and Methacrylic Acid. *Polym Composite* 30: 569–575.
24. Hegazy DE, Eid M, Madani M (2014) Effect of Ni Nano Particles on Thermal, Optical and Electrical Behaviour of Irradiated PVA/AAc Films. *Arab J Nucl Sci Appl* 47: 41–52.
25. Sapalidis AA, Katsaros FK, Kanellopoulos NK, et al. (2011) PVA/montmorillonite nanocomposites: development and properties, In: Cuppoletti J, *Nanocomposites and polymers with analytical methods*, InTech, 29–50.
26. Usuki A, Hasegawa N, Kato M, et al. (2005) Polymer-clay nanocomposites, In: *Inorganic polymeric nanocomposites and membranes*, Springer Berlin Heidelberg, 179: 135–195.
27. Părpăriţă E, Cheaburu CN, Pațachia SF, et al. (2014) Polyvinyl alcohol/chitosan/montmorillonite Nnanocomposites preparation by freeze/thaw cycles and characterization. *Acta Chem Iasi* 22: 75–96.